ACS APPLIED MATERIALS & INTERFACES

Research Article

www.acsami.org

Self-Assembly with Orthogonal-Imposed Stimuli To Impart Structure and Confer Magnetic Function To Electrodeposited Hydrogels

Ying Li,[†] Yi Liu,[‡,§] Tieren Gao,[∥] Boce Zhang,[†,⊥] Yingying Song,[†] Jessica L. Terrell,[‡,§] Nathan Barber,[‡,§] William E. Bentley,[‡,§] Ichiro Takeuchi,[∥] Gregory F. Payne,[‡,§] and Qin Wang*[,†]

[†]Department of Nutrition and Food Science, [‡]Fischell Department of Bioengineering, [§]Institute for Bioscience & Biotechnology Research, and [∥]Department of Materials Science and Engineering, University of Maryland, College Park, Maryland 20742, United States

Supporting Information

ABSTRACT: A magnetic nanocomposite film with the capability of reversibly collecting functionalized magnetic particles was fabricated by simultaneously imposing two orthogonal stimuli (electrical and magnetic). We demonstrate that cathodic codeposition of chitosan and Fe_3O_4 nanoparticles while simultaneously applying a magnetic field during codeposition can (i) organize structure, (ii) confer magnetic properties, and (iii) yield magnetic films that can perform reversible collection/assembly functions. The magnetic field triggered the self-assembly of Fe_3O_4 nanoparticles into hierarchical "chains" and "fibers" in the chitosan film. For controlled magnetic properties, the Fe_3O_4-chitosan film was electrodeposited in the presence of various strength magnetic fields and different deposition times. The magnetic properties of the resulting films should enable broad applications in complex devices. As a proof of concept, we demonstrate the reversible capture and release of green fluorescent protein (EGFP)-conjugated magnetic microparticles by the magnetic chitosan film. Moreover, antibody-functionalized magnetic microparticles were applied to capture cells from a sample, and these cells were collected, analyzed, and released by the magnetic chitosan film, paving the way for applications such as reusable biosensor interfaces (e.g., for pathogen detection). To our knowledge, this is the first report to apply a magnetic field during the electrodeposition of a hydrogel to generate magnetic soft matter. Importantly, the simple, rapid, and reagentless fabrication methodologies demonstrated here are valuable features for creating a magnetic device interface.

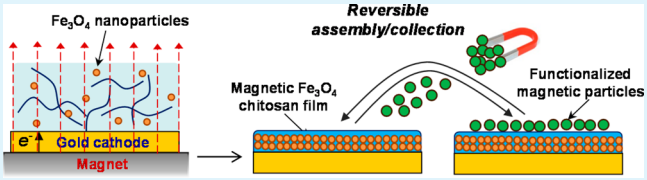

KEYWORDS: *electrodeposition, nanocomposite film, self-assembly, magnetic nanoparticles, magnetization, reversible collection, biosensor interface*

1. INTRODUCTION

Stimuli-responsive polymers that self-assemble through strong noncovalent interactions are interesting because their hierarchical structure can be controlled by a sequence of cues used to trigger self-assembly.[1,2] Once the structure is formed, the strength of the interactions precludes the structure from "annealing" to a more thermodynamically stable state. Many polysaccharides display such behavior,[3] and several studies have demonstrated that complex structures can be generated by imposing a complex sequence of triggering stimuli.[4−8]

Chitosan is a pH-responsive aminopolysaccharide that can be triggered to self-assemble to form a three-dimensional hydrogel structure. Mechanistically, chitosan's amines are protonated at low pH to yield a water-soluble cationic polysaccharide, and an increase in pH can trigger chitosan's self-assembly by a deprotonation reaction that induces a reversible sol−gel transition. Over a decade ago, chitosan was observed to electrodeposit at a cathode by the neutralization mechanism illustrated in Scheme 1a:[9−15] the imposed cathodic input yields a high pH adjacent to the cathode surface, and this serves to deprotonate chitosan's amine and induce the localized gelation of chitosan at the cathode surface.[3,16] More recent studies demonstrate that the structure[8] and properties[17] of the electrodeposited chitosan film can be controlled by the conditions used to trigger self-assembly, which is consistent with the electrodeposited hydrogel being stabilized by strong noncovalent interactions. Importantly, several groups have demonstrated that various particles can be codeposited with chitosan and entrapped within the hydrogel network. For instance, the entrapped particles could be proteins (e.g., enzymes) to confer biological function to the deposited chitosan film (e.g., for biosensing).[11,12,18] In addition, synthetic particles could be entrapped (e.g., Pt−Pb, Fe_3O_4, MnO_2, and Au nanoparticles) to confer electrical function to the film (e.g., to facilitate signal transduction).[6,19−22]

Here, we report the use of two orthogonal-imposed stimuli to self-assemble a composite film with magnetic properties. As illustrated in Scheme 1b, we first suspend magnetic Fe_3O_4 nanoparticles (MNPs) in a chitosan solution and then impose an electrical input to trigger chitosan's cathodic electrodeposition. During deposition, we simultaneously impose a magnetic signal that serves to organize the Fe_3O_4 nanoparticles.

Received: March 17, 2015
Accepted: April 29, 2015
Published: April 29, 2015

DOI: 10.1021/acsami.5b02339
ACS Appl. Mater. Interfaces 2015, 7, 10587−10598

Scheme 1. (a) Mechanism of Co-Electrodeposition of pH-Responsive Chitosan and Magnetic Nanoparticles at a Cathode; Entrapped Particles Are Randomly Distributed within the Film When Co-Deposition Is Performed in the Absence of an Applied Magnetic Field. (b) Simultaneous Imposition of a Magnetic Field During Co-Deposition Can (i) Organize Structure, (ii) Confer Magnetic Properties, and (iii) Yield Magnetic Films That Can Perform Reversible Assembly/Collection Functions

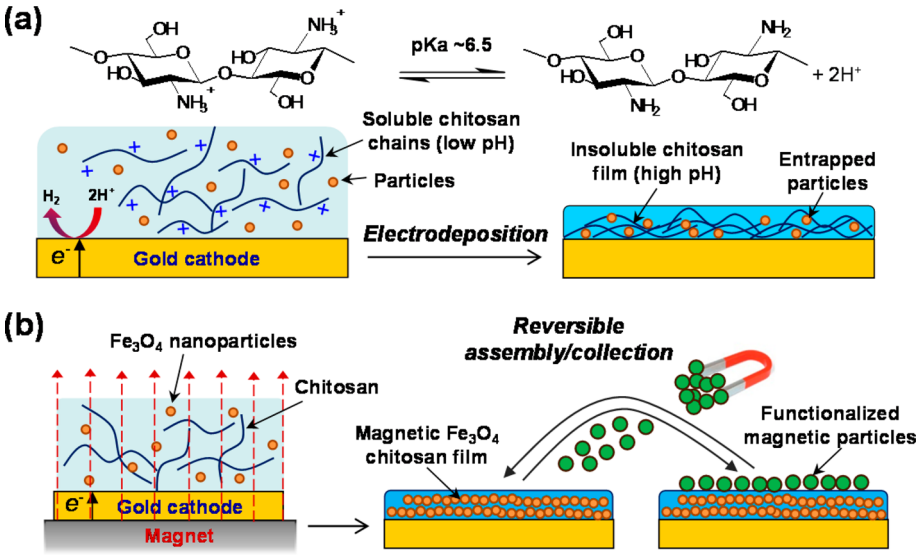

Specifically, we demonstrate that electrodeposition in the presence of an imposed magnetic field: (i) organizes the hierarchical structure of the nanoparticles within the electrodeposited chitosan hydrogel film, (ii) confers magnetic properties to the film, and (iii) yields magnetic films that can reversibly capture biologically based magnetic particles.

2. EXPERIMENTAL SECTION

2.1. Preparation of Cast MNP-Chitosan Film. Chitosan solution (1% w/w, pH 5.3) was prepared as previously reported.[3] The synthesis of amine-functionalized MNPs was reported by Wang et al.[23] The detailed synthetic procedures and characterization of the MNPs can be seen in the Supporting Information.

The MNP-chitosan suspension was prepared by sonicating and vortexing 10 mg of MNPs in 10 mL of chitosan solution for 30 min and then casting on a piece of aluminum sheet under which was placed a magnet disc. The cast MNP-chitosan film was then dried under ambient conditions under the influence of the imposing magnetic field from the magnet disc. Three types of N48 neodymium magnets (Apex Magnets, Petersburg, WV) were used, namely, 1.27 d × 0.318 h cm disc, 1.27 d × 0.635 h cm disc, and 1.27 d × 1.27 h cm cylinder. The distance between the magnets and the aluminum sheet was adjusted using nonmagnetic material to obtain the target magnetic field strength that was measured by a hand-held gaussmeter (model 410, Lake Shore Cryotronics, Inc.). Cast MNP-chitosan films without applying an external magnetic field were prepared as a control.

2.2. Electrodeposition of Chitosan and MNP-Chitosan Films. A piece of 5 mm thick polydimethylsiloxane (PDMS) with a punched hole (8 mm in diameter) was placed on top of a gold coated quartz electrode (International Crystal Manufacturing) and assembled with or without a magnet under the electrode. A 200 μL chitosan solution (1.0%, pH 5.3) or MNP-chitosan suspension (0.8 mg MNPs/ml) was pipetted on top of the gold electrode, and a Pt wire counter electrode was immersed into the deposition solution. Electrodeposition was initiated by biasing the gold electrode as a cathode using a DC power source (2400 Sourcemeter, Keithley Instruments, Inc.). Detailed information about the deposition time and applied magnetic field is provided in the text.

2.3. Characterization of MNP-Chitosan Films. The experimental procedures for X-ray diffraction crystallography analysis are provided in the Supporting Information.

Scanning electron microscopy (SEM) images were obtained from a Hitachi SU-70 SEM microscope. Film samples were adhered to a 1 in. specimen stub with conductive carbon tape (Electron Microscopy Sciences). A thin layer of gold and platinum was then coated on the samples using a sputter coater (Hummer XP). Energy dispersive X-ray (SEM-EDS) mapping was obtained using a Bruker SOL-XE detector (Bruker AXS Inc.). In SEM-EDS spot analysis, representative points in the elemental map were randomly selected to investigate the elemental composition. The distribution of four elements (C, N, O, and Fe) and their relative content in samples were reported.

Magnetic properties of MNPs, MMPs, and MNP-chitosan films were measured by a vibrating sample magnetometer (VSM, 7400, Lake Shore Cryotronics, Inc.). The powdered MNPs and MMPs were filled inside a Kel-F sample holder cup (Lake Shore Cryotronics, Inc.). The film-coated gold electrodes or aluminum sheets were attached to a Kel-F thin-film bottom sample tail (Lake Shore Cryotronics, Inc.) by cellophane tape. All experiments were conducted at 25 °C.

2.4. Conjugation of Protein and Antibody to MMPs. Preparation and purification of enhanced green fluorescent protein (EGFP) has been reported previously.[24] Briefly, recombinant *Escherichia coli* (*E. coli*, BL21(DE3)) bearing pET-eGFP-7K (kanamycin-resistant plasmid) was used for the production of His-tagged EGFP. Extraction of EGFP and purification using His affinity agarose Co-NTA Agarose (Cube Biotech) were performed following the product protocols. For conjugation of antibody to MMPs, polyclonal *E. coli* serotypes O + K antibody (Goat/IgG, PA1–27226, Pierce Biotechnology, Inc.) was used.

EGFP or antibody was conjugated on MMPs through carboxyl activating agent 1-ethyl-3-(3-(dimethylamino)propyl) carbodiimide (EDC). The reaction was carried out in 2-(*N*-morpholino)-ethanesulfonic acid (MES) buffer. First, 1 mg of MMPs, 300 μL of MES (pH 5.2), and 35 μL of EDC solution (2 mg/mL in pH 5.2 MES buffer) were mixed for 30 min, and then the activated MMPs were separated from the liquid by applying a magnet to the container. Second, the activated MMPs were mixed with 150 μL of EGFP solution (1 mg/mL in pH 7.2 MES buffer) or 100 μL of *E. coli* antibody solution (1 mg/mL in pH 7.2 PBS buffer) in the dark at 25 °C for 4 h. Finally, the resulting MMP-EGFP or MMP-antibody conjugates were magnetically separated and resuspended in 1 mL of MES buffer (pH 7).

2.5. Statistical Analysis. All measurements were carried out in triplicate. The results are expressed as means. For statistical analysis, the data were subjected to analysis of variance ($P < 0.05$) followed by

DOI: 10.1021/acsami.5b02339
ACS Appl. Mater. Interfaces 2015, 7, 10587–10598

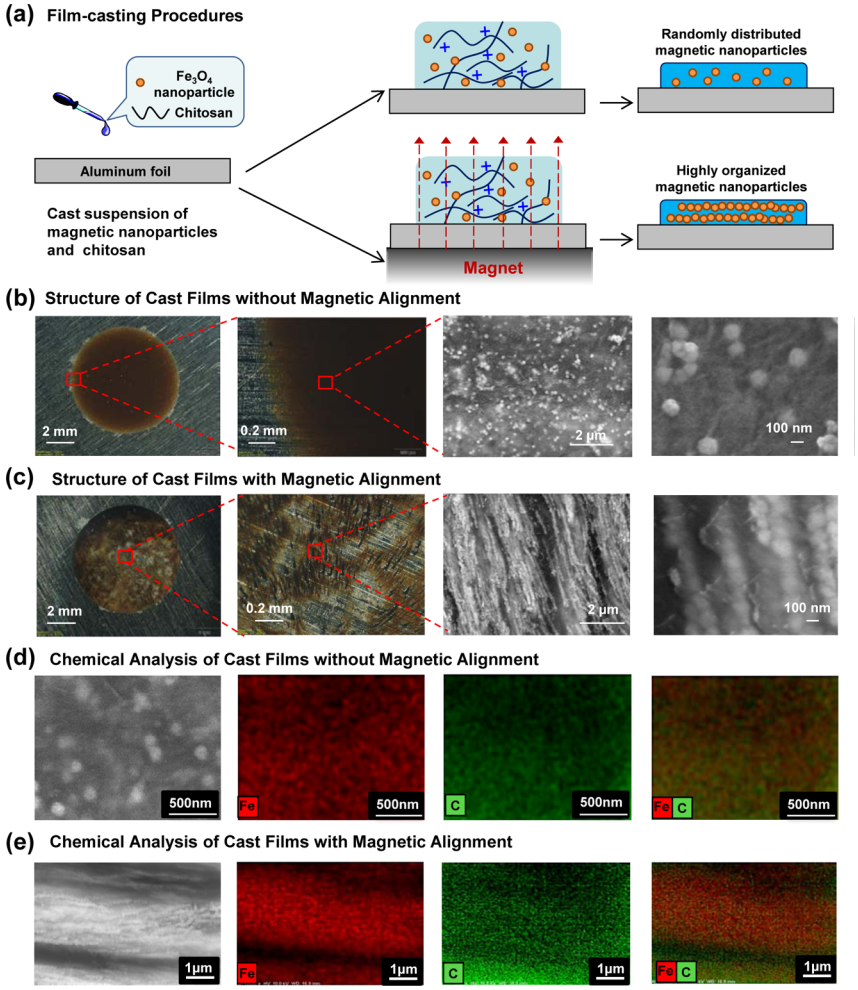

Figure 1. (a) Schematic illustration of film-casting procedures in the presence/absence of an applied magnetic field. (b) Structure of cast films without magnetic alignment. (c) Structure of cast films with magnetic alignment. (d) Chemical analysis of cast films without magnetic alignment. (e) Chemical analysis of cast films with magnetic alignment. The images were taken in top-down view by optical microscopy and SEM.

Tukey's test with an experiment-wise confidence level of $\alpha = 0.10$ using SAS 9 software (SAS Institute Inc.).

3. RESULTS AND DISCUSSION

3.1. Casting MNP-Chitosan Films: Alignment of Magnetic Nanoparticles. *3.1.1. Structural Evidence of Magnetic Alignment of MNPs in the Cast Film.* In our initial tests, we examined the effect of an external magnetic field on MNPs in a cast chitosan film. Figure 1a schematically illustrates the MNP-chitosan film casting procedures in the presence/absence of an applied magnetic field. The MNP-chitosan film in the presence of a magnetic field was prepared by dropping 20 μL of well-suspended MNPs (1 mg/mL) in chitosan solution (1%, pH 5.3) on an aluminum sheet that has a magnet disc underneath. The cast MNP-chitosan film was allowed to dry at room temperature overnight with the magnetic field applied during the whole process. The control film was prepared in the same way except no magnetic field was applied.

Figure 1b shows the structure of the cast MNP-chitosan film without magnetic alignment. The two left images are photographs of the cast film showing uniformly distributed MNPs in chitosan. The SEM images on the right side of Figure 1b show that the discrete MNPs were randomly embedded in the film. On the other hand, MNP-chitosan films cast in the presence of a magnetic field showed highly ordered patterns. The photographs on the right of Figure 1c show uneven distribution of MNPs in the film. The SEM images in Figure 1c show groups of fiberlike structures, and almost all of the MNPs in the films were completely aligned into chains without disorderly located ones. The magnified SEM image (right most panel in Figure 1c) shows that the fibers were composed of straight necklacelike chains that consisted of spherical MNPs. The texture of the chitosan layer can also be seen on top of the MNP chains, suggesting that the MNP chains were pulled away from the surface and embedded deeper into the chitosan film.

3.1.2. Chemical Evidence of Magnetic Alignment of MNPs in the Cast Film. The effect of the external magnetic field on the MNP alignment in the chitosan film can also be examined using SEM-EDS elemental mapping analysis. Figure 1d shows that the MNP-chitosan film without magnetic alignment has homogeneous distributions of iron and carbon. This suggests that the MNPs were well dispersed in the film and that the magnetic moments of the MNPs in the film were randomly oriented.

Figure 1e shows that the MNP-chitosan film with magnetic alignment has enriched areas of iron and carbon. The distribution of iron corresponds to the presence of MNP chains seen in the SEM image on the left. The widespread signal of carbon suggests that the layout of chitosan covered the most area in the film. Taken together, Figure 1 demonstrates

DOI: 10.1021/acsami.5b02339
ACS Appl. Mater. Interfaces 2015, 7, 10587−10598

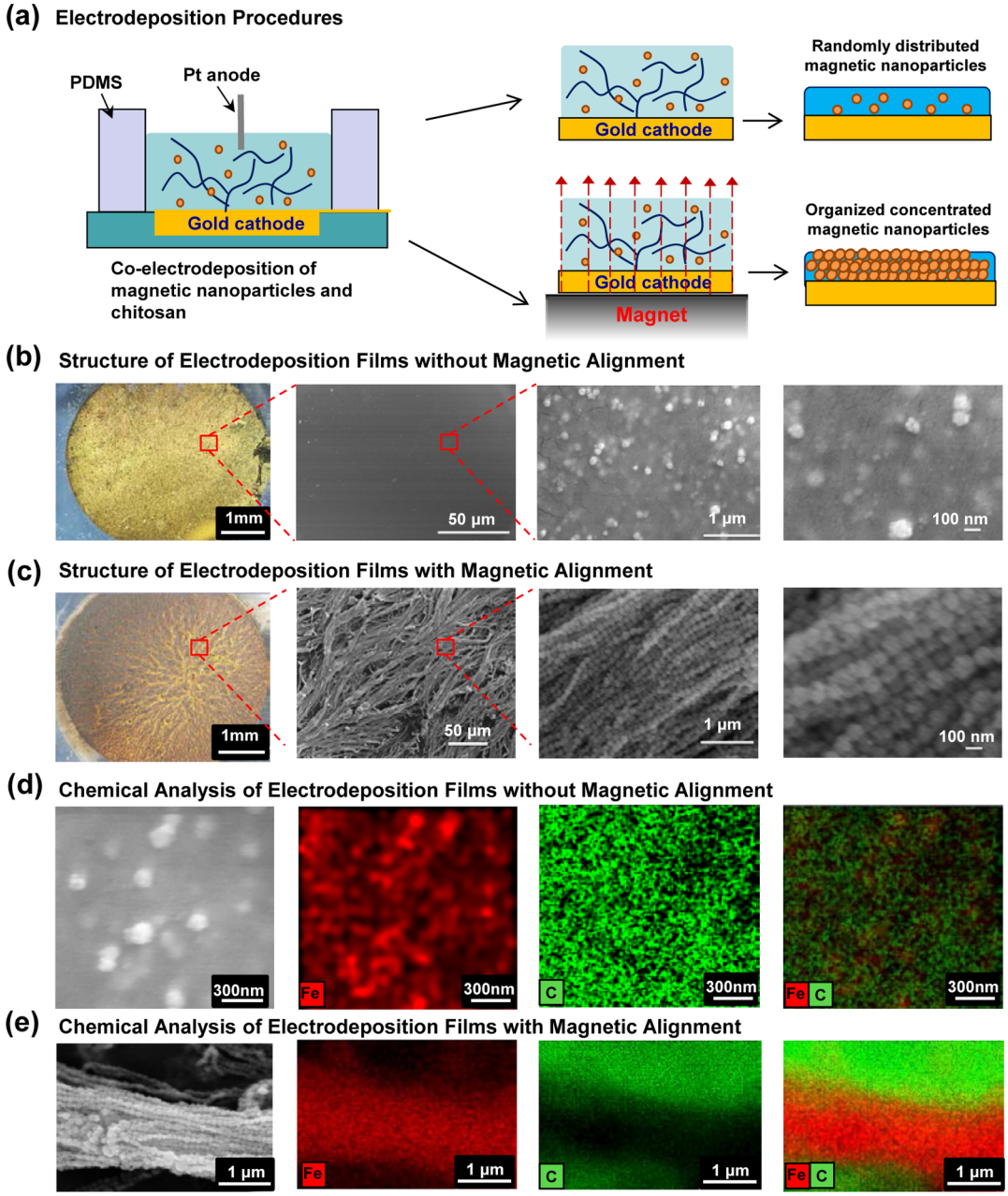

Figure 2. (a) Schematic illustration of film electrodeposition procedures in the presence/absence of a magnetic field. (b) Structure of electrodeposited films without magnetic alignment. (c) Structure of electrodeposited films with magnetic alignment. (d) Chemical analysis of electrodeposited films without magnetic alignment. (e) Chemical analysis of electrodeposited films with magnetic alignment. The images were taken in top-down view by optical microscopy and SEM.

that an external magnetic field can trigger the self-assembly of MNPs into long-range ordered chains and further created hierarchical parallel clusters of the assembled chains over large areas in the chitosan film. The linking of the MNPs was possibly driven by magnetostatic interactions.[25]

3.2. Electrodeposition of MNP-Chitosan Film: Simultaneous Application of Electrical Stimuli and Magnetic Field. *3.2.1. Electrodeposition of MNP-Chitosan Film.* Electrodeposition of chitosan films showed unique advantages in creating microdevices in that this directed assembly process can be controlled spatially and temporally.[26] To coelectrodeposit MNPs and chitosan, we assembled the gold-coated quartz electrode as schematically illustrated in Figure 2a and exposed it to an MNP-chitosan suspension. For magnetic alignment experiments, a magnet was placed under the electrode to create a magnetic field. Because the electrode was centered and much smaller than the magnet, the direction of the applied magnetic field could be considered out of plane. Electrodeposition was initiated by applying a constant current density of 3 A/m^2 to the gold cathode for 4 min in the presence of the magnetic field. After electrodeposition, the film was gently rinsed with water to remove undeposited materials and air-dried overnight in ambient conditions. The magnet was removed after the films were dried. Control films were prepared without using magnets during the entire process.

3.2.2. Structural Evidence of Magnetic Alignment and Increased Accumulation of MNPs in MNP-Chitosan Films during Electrodeposition. Electrodeposited MNP-chitosan

DOI: 10.1021/acsami.5b02339
ACS Appl. Mater. Interfaces 2015, 7, 10587−10598

films without magnet alignment were observed to be translucent with scattered black particles (left photograph in Figure 2b). SEM images in Figure 2b show a homogeneous distribution of spherical MNPs in the film, indicating that these particles were well dispersed without aggregation. This is consistent with the cast MNP-chitosan film prepared without applying an external magnetic field. Presumably, the magnetic moments of MNPs are randomly oriented in the film.

On the other hand, electrodeposited MNP-chitosan films with magnetic alignment display dramatic structural difference compared to those deposited without alignment. Films with magnetic alignment (left photograph in Figure 2c) were much darker than those without magnetic alignment (Figure 2b), indicating more MNPs were deposited in the presence of the external magnetic field, presumably due to magnetic attraction between MNPs and the magnet under the electrode. SEM images in Figure 2c show crowded "fibers", which consisted of MNP chains throughout the film. Magnified SEM images in Figure 2c clearly show that MNPs form highly ordered parallel chains and that the particles themselves orient along the chain.

3.2.3. Chemical Evidence of Magnetic Alignment and Concentration of MNPs in MNP-Chitosan Films during Electrodeposition. SEM-EDS analysis provided chemical evidence for the coelectrodeposition of MNPs and chitosan and the significant aligning effect of the magnetic field during electrodeposition. Figure 2d shows that without magnetic alignment during the electrodeposition the iron signals are randomly distributed throughout the films, indicating good dispersion of MNPs in the film. Carbon signals are also uniformly distributed, corresponding to the observation that MNPs are randomly embedded in the chitosan film in the nonaligned cases. On the other hand, Figure 2e shows that strong iron signals coincide with the MNPs fibers as shown in the SEM image on the left side for the electrodeposited MNP-chitosan film with magnetic alignment. In addition, carbon signals dominate areas other than the dense MNP fibers, indicating that these fibers were on the surface of the film or replaced chitosan.

For the evaluation of variations in the amounts of MNPs in the MNP-chitosan films, SEM-EDS elemental quantitative analysis was conducted by randomly probing various spots in the examined SEM area; the results are shown in Table 1. The amount of MNPs in the suspension for casting the film was the same in the presence or absence of magnetic field; thus, it is not surprising that the relative atomic ratios of iron in both films were reasonably close to each other. On the other hand, the iron ratio in the electrodeposited film with magnetic alignment was remarkably higher than that in the film without magnetic alignment, providing chemical evidence for the enrichment effect of the magnetic field on the assembly of MNPs in the chitosan film during the electrodeposition process.

Table 1. SEM-EDS Analyses of Normalized Average Atomic Ratio (%) of C, N, O, and Fe in the MNP-Chitosan Films Fabricated by Electrodeposition or Casting in the Presence or Absence of a Magnetic Field (MF)[a]

element	electrodeposited film without MF	electrodeposited film with MF	casting film without MF	casting film with MF
C	31.4 ± 8.5	22.1 ± 0.9	35.0 ± 2.6	31.2 ± 1.7
N	28.6 ± 9.2	17.3 ± 0.8	23.9 ± 2.2	18.4 ± 1.3
O	39.6 ± 14	30.9 ± 1.57	29.6 ± 2.6	35.1 ± 2.3
Fe	0.25 ± 0.10	29.7 ± 0.2	11.5 ± 0.1	15.3 ± 0.4

[a]Data are expressed as mean percentage ± standard error of the mean.

3.3. Control of the Magnetic Properties of the Film during the Deposition Process. *3.3.1. Magnetic Properties of Cast MNP-Chitosan Films.* Magnetic properties of magnetic materials are often evaluated by hysteresis loops,[27] which can be obtained from a vibrating sample magnetometer. From the hysteresis loops, one can obtain (1) saturation magnetization (M_s), which represents a state where an increase in applied external magnetic field cannot further increase the magnetization of the material; (2) remanent magnetization (M_r), which indicates how much magnetization has been retained when the externally applied field is brought to zero after magnetic saturation has been attained; and (3) coercivity. In addition, the value of M_r/M_s, the squareness ratio, measures how square a hysteresis loop is, which reflects the easy/hard trend of magnetization reversal. Hysteresis measurements of our MNP-chitosan films were recorded with a static magnetic field applied either parallel (in-plane) or normal (out-of-plane) to the plane of the film. The value of M_s was considered as in-plane magnetization measured at magnetic field of 3 kOe. As shown in Figure S2a in the Supporting Information, the representative in-plane and out-of-plane hysteresis loops of the film cast with 3.5 kOe indicate that the easy axis of the film lies in the film plane, which is consistent with other thin films containing iron or magnetite.[25,28]

First, to investigate the effects of magnetic alignment on the magnetic properties of cast MNP-chitosan films, we compared in-plane hysteresis loops of cast MNPs-chitosan films with or without magnetic alignment. As shown in Figure 3a, M_s of the film with magnetic alignment (3.5 kOe field) is slightly higher (~6%) than that of the film without magnetic alignment. Importantly, the M_r of a cast MNP-chitosan film with magnetic alignment is much higher (2-fold) than that without magnetic alignment, indicating that the magnetic moments of MNPs in the cast film are partially aligned in the film plane.

Next, we investigate whether the magnetic properties of the MNP-chitosan film are tunable by varying the strength of the applied magnetic field. The M_s of all of the aligned films did not vary significantly (data not shown). Figure 3b shows M_r and M_r/M_s measured in the film plane, and Figure 3c shows those measured out of the film plane. It can be seen that the M_r and M_r/M_s measured in-plane increase as a function of applied magnetic field during casting and are remarkably larger than those measured out-of-plane, even though the magnetic field was applied out of the film plane. We offer the following explanation about the results in Figure 3b and c.

Commonly, the magnetic moments of magnetic materials tend to align along the applied field.[29−32] For an individual particle, its magnetic energy is the lowest when the magnetic moment is oriented along the applied field direction.[33] However, because the easy axis of the MNP chains lay in-plane, altering the direction of their magnetic moments to the out-of-plane direction mean that the strength of the applied magnetic field has to overcome the sum of the demagnetization field, chain−chain interactions field, and magnetocrystalline anisotropy field. The demagnetization field is expressed as[34]

$$H_d = -N_d M$$

where N_d is the global demagnetizing factor, and M is the magnetization of the MNPs. N_d is equal to 1 along the chain direction for chains embedded in a thin film.[34] The demagnetization field was evaluated to be 4.5 kOe using

DOI: 10.1021/acsami.5b02339
ACS Appl. Mater. Interfaces 2015, 7, 10587−10598

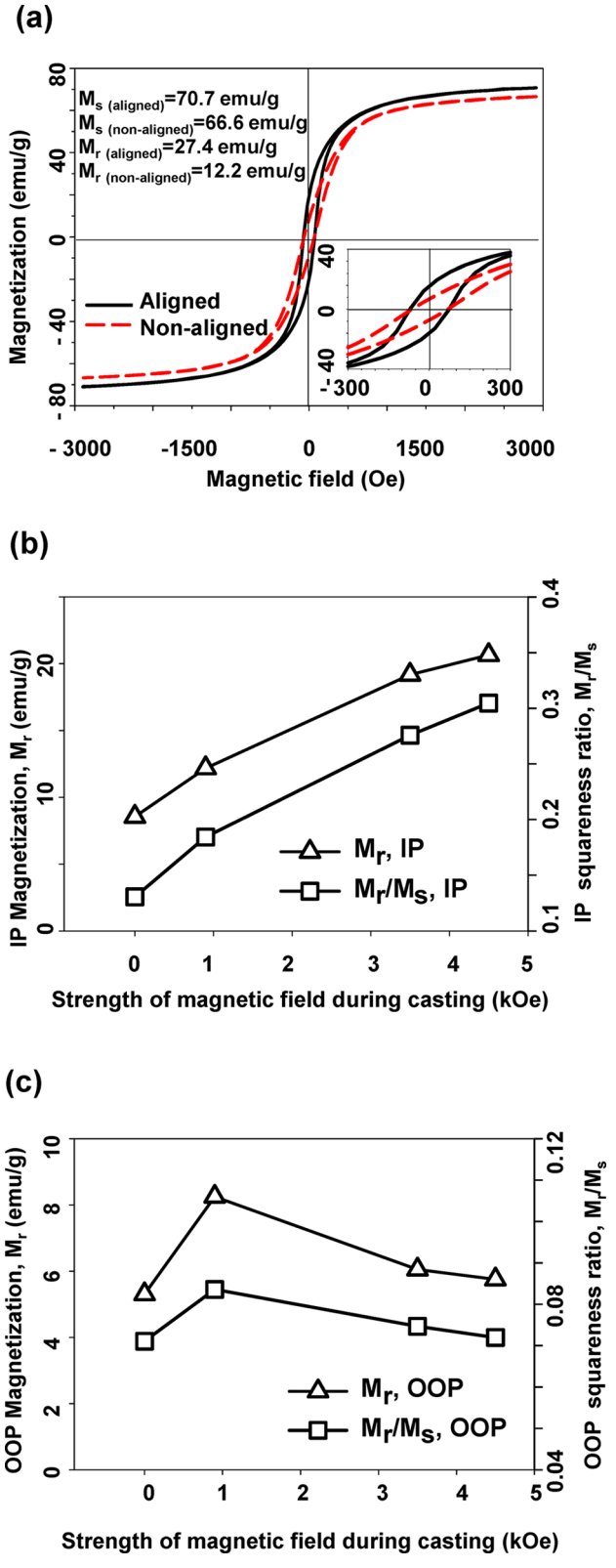

Figure 3. (a) Representative hysteresis loops of cast MNP-chitosan films with (solid line) or without (dash line) magnetic alignment (3.5 kOe field) measured parallel to the film plane. The inset represents higher magnification detail of the hysteresis loops in the low field region. The (b) in- and (c) out-of-plane remanence (M_r) and squareness ratio (M_r/M_s) of cast films as a function of the strength of the external magnetic field. The amount of MNPs was 20 μg in all of the films. IP, in-plane; OOP, out-of-plane.

magnetization of 354 emu/cm^3 with a density of Fe_3O_4 of 5 g/cm^3. Second, the magnetostatic interactions among particles and chains greatly increases the difficulty of domain rotation.[25] Therefore, the force needed to orient the magnetic moments to the out-of-plane direction was speculated to be far greater than 4.5 kOe, which was the largest field strength applied in this study. Third, magnetocrystalline anisotropy might contribute to the easy axis alignment, although it is small.[35] In summary, an applied field must exceed a certain critical value for irreversible rotation of the magnetic moment to occur.[36] Therefore, it was favorable for the MNP chains to align in the film plane despite the fact that the direction of the applied field was perpendicular to the film plane.

For films cast in a 1 kOe field, the M_r and M_r/M_s measured in both directions were significantly higher than that of the nonaligned film (Figure 3b and c), probably because the MNPs were magnetized and self-assembled into ordered structures for the aligned films. Interestingly, in the range of 1−4.5 kOe, the M_r and M_r/M_s in the plane of the films increased as a function of magnetic field strength, whereas those parameters of the film measured in the out-of-plane direction decreased. The value of out-of-plane M_r and M_r/M_s of the films cast in a 4.5 kOe field decreased to almost the same as those of nonaligned films. This trend suggested that the cast MNP-chitosan film was more easily magnetized along the film plane with increasing field. In addition, increasing the field strength may have an impact on aligning the easy axis of the MNP chains to a certain direction within the plane.

3.3.2. Magnetic Properties of Electrodeposited MNP-Chitosan Films. 3.3.2.1. The Effect of an External Magnetic Field on the Magnetic Properties of Electrodeposited Films. Electrodeposited MNP-chitosan films were prepared by adding the MNP-chitosan suspension (0.8 mg/mL in 1.0% chitosan) on top of the gold electrode, and electrodeposition was initiated by biasing the gold electrode as a cathode (3 A/m^2) for 4 min. During the deposition and subsequent washing and drying, magnetic discs with varying magnetic field strength were placed under the gold electrode to tune the magnetic field. Unlike the cast MNP-chitosan films, the amount of MNPs in deposited films depends on the deposition conditions. Therefore, the total magnetic moments (m_r and m_s) were used to evaluate the effects of strength of the external magnetic field on the magnetic properties of the films. The value of m_s was considered an in-plane magnetic moment measured at 3 kOe. As shown in Figure 4a, m_s of the films increased as a function of the strength of the external magnetic field, indicating that more MNPs were deposited on the electrode surface upon increasing the magnetic field strength of the magnetic disc.[37]

Figure 4b shows that the in-plane m_r of the films increased almost linearly with the strength of the applied magnetic field, whereas out-of-plane m_r remained nearly constant. Also, the in-plane m_r of the films deposited in the presence of a 1−4 kOe magnetic field was significantly higher than that of the corresponding out-of-plane m_r, probably due to the predominant alignment of the MNP chains in the film plane. This is consistent with our observation for the cast MNP-chitosan films (Figure 3b and c). The increased in-plane m_r might arise from the combination effects of (1) an increased amount of MNPs electrodeposited on the electrode surface and (2) more magnetic moments of the MNPs aligned toward a certain direction in the plane. Because the easy axis of the electrodeposited film was in-plane (Figure S2b, Supporting Information), the limited increase in the out-of-plane m_r was

DOI: 10.1021/acsami.5b02339
ACS Appl. Mater. Interfaces 2015, 7, 10587−10598

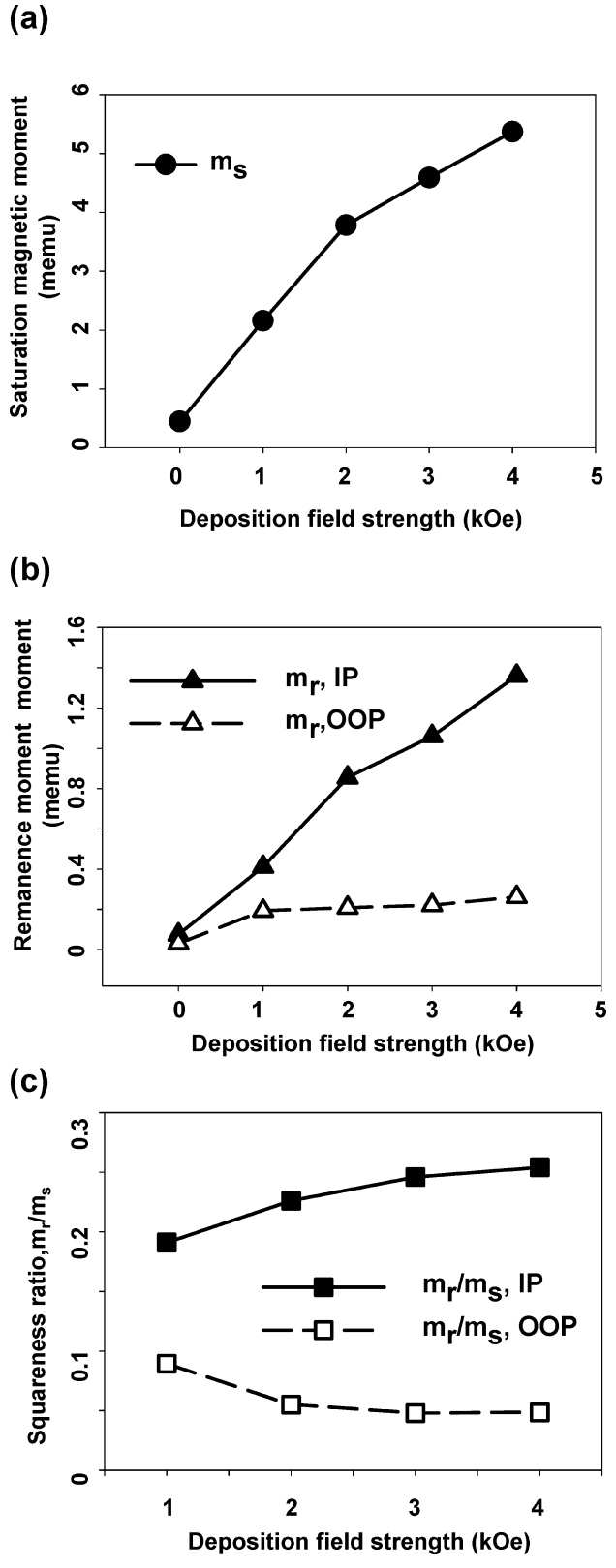

Figure 4. (a) Total saturation magnetic moment (m_s) of an electrodeposited film as a function of the strength of the applied magnetic field. (b) The remanence moment (m_r) of an electrodeposited film in the in-plane and out-of-plane direction as a function of the strength of an external magnetic field. (c) The squareness ratio (m_r/m_s) of electrodeposition films as a function of the strength of an external magnetic field. IP, in-plane; OOP, out-of-plane.

probably due to difficulty in reversing the magnetic moments from in-plane to out-of-plane, as demonstrated for the cast films (section 3.3.1).

Figure 4c shows that the applied magnetic field differentially impacted the in-plane and out-of-plane m_r/m_s of the electrodeposited films. Because m_r/m_s is a normalized value, we showed that the trend of m_r/m_s was indeed independent of the amount of MNPs in the film. It was obvious that when increasing the strength of the magnetic field, the in-plane m_r/m_s increased whereas the out-of-plane m_r/m_s decreased. This phenomenon was consistent with our observation for the cast films (Figure 3b and c), suggesting that the electrodeposited MNP-chitosan film was more easily magnetized and directionally aligned in the film plane with increasing field. This also contributed to the increase of in-plane m_r upon increasing the strength of the external magnetic field as shown in Figure 4a. In summary, adjusting the strength of the magnetic field during electrodeposition resulted in tuning of magnetic properties of the electrodeposited MNP-chitosan films in both in-plane and out-of-plane directions.

3.3.2.2. The Effect of Deposition Time on Magnetic Properties of Electrodeposited Films. The unique feature of electrodeposition of chitosan lies in the fact that electrodeposited films can be spatiotemporally controlled.[38] Here, we examine the effect of deposition time[3,17] on the magnetic properties of the MNP-chitosan films. The MNP-chitosan films were prepared by electrodepositing (3 A/m^2) an MNP-chitosan solution (0.8 mg/mL) for 1−4 min in the presence of a magnetic field (1 kOe). Panels a and b in Figure 5 show that the m_s, in-plane m_r, and out-of-plane m_r of the MNP-chitosan film increase as a function of deposition time. Because the thickness of the electrodeposited chitosan film depends on the deposition time,[3,9,16] more MNPs could be incorporated into the chitosan film over time, resulting in increased m_s and m_r in both in-plane and out-of-plane directions for the film. However, m_r/m_s remain nearly constant for varied deposition times (Figure 5c), possibly because this parameter mainly responds to the strength of a magnetic field.

In summary, Figures 3, 4, and 5 demonstrate that magnetic properties of the MNP-chitosan films can be tuned by adjusting the strength of the magnetic field during film preparation processes.

3.4. Magnetic Interactions between Functionalized Magnetic Particles and MNP-Chitosan Films. The assembly/collection of biomaterial-conjugated magnetic microparticles (MMPs) by the magnetically aligned MNP-chitosan film was performed to demonstrate its reversible application.

3.4.1. Magnetic Attractions Between MMP-EGFP and a Cast MNP-Chitosan Film. We performed initial studies using cast films to demonstrate the magnetic attractions between MMPs and MNP-chitosan films. Because the total magnetic moments (m_s and m_r) of the MNP-chitosan films are sensitive to the concentration of MNPs, the use of cast films precludes differences due to MNP concentration.

First, carboxyl-functionalized MMPs were synthesized by a hydrothermal reaction of ferric ammonium citrate, hydrazine monohydrate, and poly(acrylic acid).[39] The size, composition, and magnetic properties of the MMPs can be found in Figure S1b, d, and e, respectively, in the Supporting Information. Second, EGFP was conjugated on MMPs through the carboxyl activating agent EDC (see Experimental Section 2.4). Successful conjugation of EGFP to the MMPs is shown in Figure S3 in the Supporting Information. Third, three cast films

DOI: 10.1021/acsami.5b02339
ACS Appl. Mater. Interfaces 2015, 7, 10587−10598

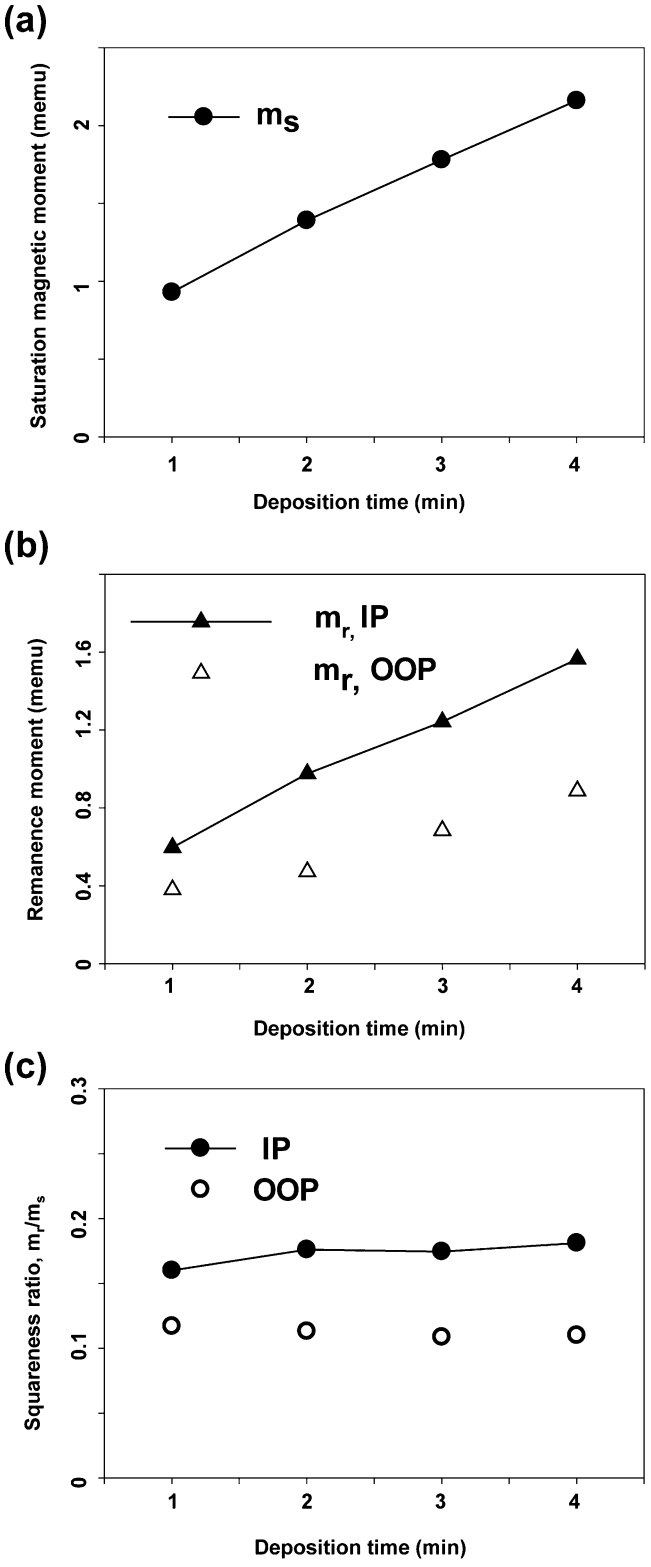

Figure 5. Effects of deposition time on the (a) m_s, (b) m_r, and (c) m_r/m_s of the MNP-chitosan films electrodeposited in the presence of a magnetic field of 1 kOe. IP, in-plane; OOP, out-of-plane.

were prepared by dropping 20 μL of corresponding solution onto a metal substrate. During film formation, the MNP-chitosan film (cast using 2 mg/mL MNP in chitosan suspension) with magnetic alignment was exposed to a magnetic field of 1 kOe, whereas the film without magnetic alignment was not exposed to an external magnetic field. A chitosan-only film was also prepared. As shown in Figure 6a,

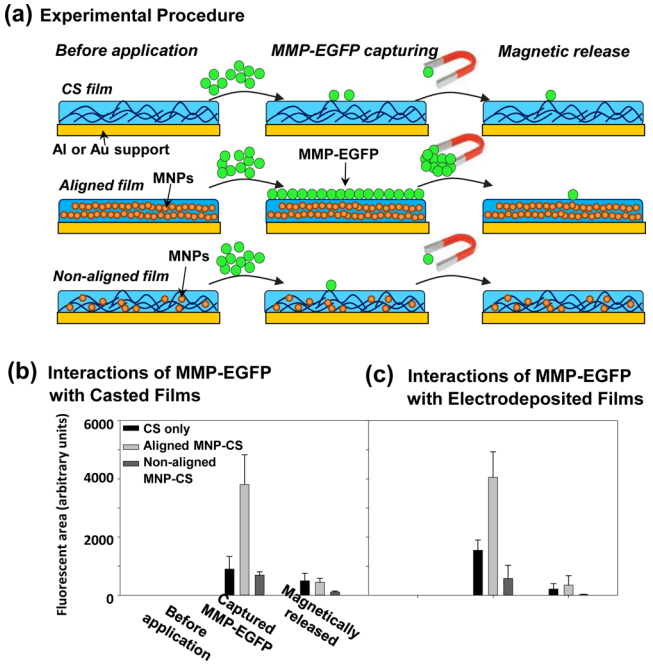

Figure 6. (a) Schematic illustration of experimental procedures for imaging magnetic interactions between EGFP-MMPs and the films. Both cast and electrodeposited films were tested following these procedures. (b) Interactions between MMP-EGFP and cast films. (c) Interactions between MMP-EGFP and electrodeposited films. The results were expressed as means ± standard deviation (n = 3). Representative fluorescence microscopic images of (b) and (c) are shown in Figure S4 in the Supporting Information. CS, chitosan.

the MMP-EGFP suspension (60 μL) was flowed on the magnetically aligned film, the nonaligned film, and the chitosan only film. After 30 s of contact, the films were rinsed with deionized water 3 times. Images of these films were taken using a GFP filter on an Olympus MVX10 MacroView microscope equipped with an Olympus DP72 digital camera. Representative fluorescence microscopic images of these films after each treatment are shown in Figure S4 in the Supporting Information. The fluorescent area of each film was analyzed by ImageJ software (rsb.info.nih.gov/ij) using the same color threshold.

Figure 6b shows that the total fluorescent area (i.e., working signal) of the magnetically aligned film was 4.2 and 5.5 times higher than that of the chitosan and nonaligned films, respectively. This is expected because MMP-EGFP was attracted by the magnetically aligned MNP-chitosan film but not the nonaligned or chitosan-only films. We provide the following explanations. First, the higher value of M_r of a magnetic film indicates that higher magnetic energy is stored in the film to attract the magnetic materials around it by magnetic force.[40] As discussed in section 3.3.1, the MNP-chitosan film with magnetic alignment had a higher M_r than the one without magnetic alignment. Second, because the MNP-chitosan film without magnetic alignment was not exposed to a magnetic field during preparation, the MNPs in the film were not magnetized; thus, the magnetic fields generated by these particles were very weak and pointed in different directions. Therefore, although there is an M_r value for the nonaligned

DOI: 10.1021/acsami.5b02339
ACS Appl. Mater. Interfaces 2015, 7, 10587−10598

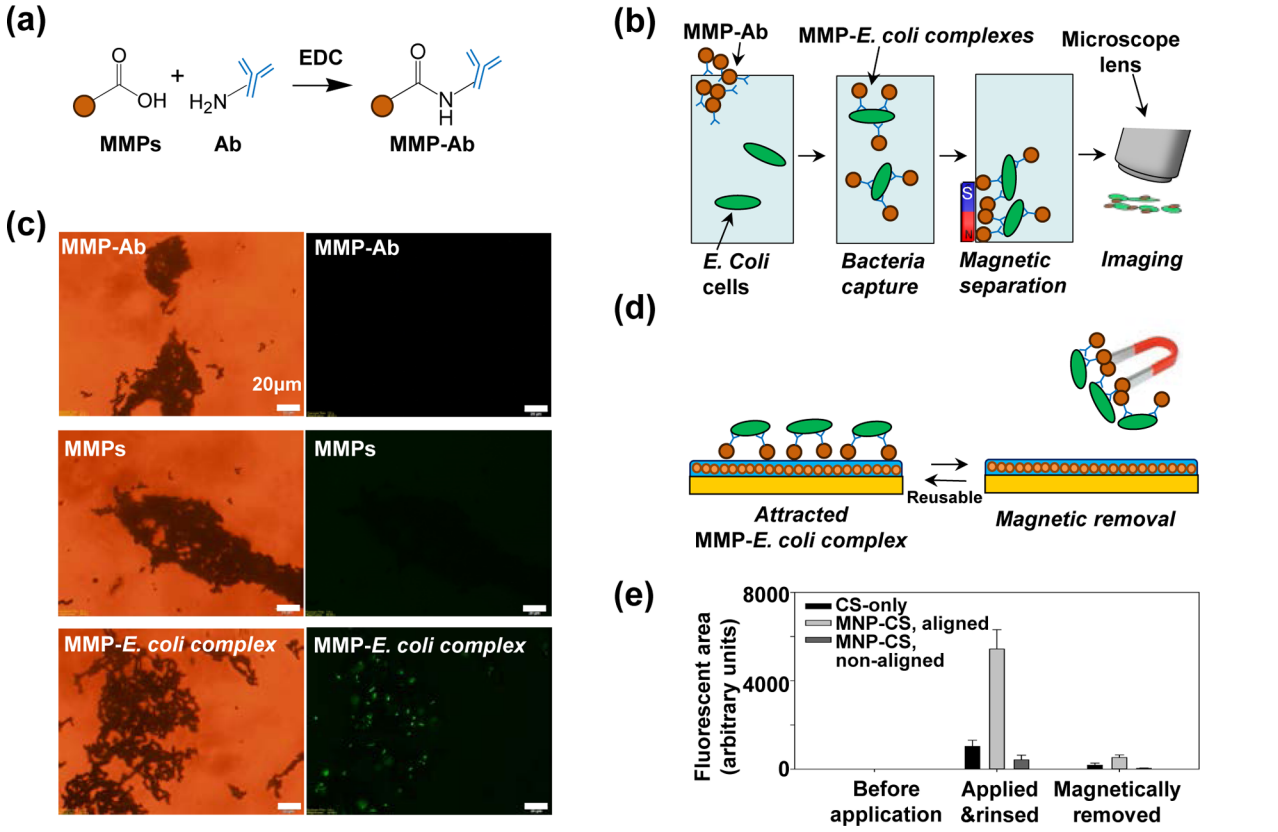

Figure 7. (a) Conjugation reaction of MMPs and antibody to form MMP-antibody conjugates using the EDC method. (b) Experimental procedures for immunomagnetic separation of *E. coli* by MMP-antibody. (c) *E. coli* cells (fluorescently stained) were captured by MMP-antibody conjugates but had little affinity for nonconjugated MMPs. The upper panels are the bright field and fluorescence microscopic images of MMP-antibody conjugates without adding *E. coli*. The middle and lower panels show the rinsed nonconjugated MMPs and MMP-antibody after adding *E. coli*, respectively. (d) Schematic illustration of the collection and magnetic release of MMP-*E. coli* complexes on the aligned MNP-chitosan films. (e) Magnetic interactions of MMP-*E. coli* complexes with MNP-chitosan films with or without magnetic alignment and with the chitosan-only film. The results were expressed as means ± standard deviation (n = 3). CS, chitosan; Ab, antibody.

films, their attraction to MMPs was not higher than that of the chitosan only (nonmagnetic) film.

3.4.2. Magnetic Removal of MMP-EGFP from the Cast MNP-Chitosan Film. To release the MMP-EGFP from the MNP-chitosan films (Figure 6a, right side), the magnetically aligned, nonaligned, and chitosan-only films were immersed in water. A neodymium magnet was placed at a distance of 5 mm from the film for 5 min. The films were taken out for fluorescent imaging using the same microscope described in section 3.4.1. As shown in the right most set of columns in Figure 6b, after magnetic removal of EGFP-MMPs, the fluorescent signal of the magnetically aligned film was reduced to 11.7% of that of its working signal and was not significantly different from that of the chitosan only film. This provided further evidence that the binding of MMP-EGFP and the aligned film was mainly through magnetic attraction. It is worth noting that magnetic removal of MMPs from the MNP-chitosan film using an external magnet did not disturb the alignment or magnetic field of the film because (1) the magnetic moment of the MNPs will return to the original direction (easy axis) once the external magnetic field is removed because, as discussed in section 3.3.1, the applied field did not exceed the critical value for irreversible rotation of magnetic moment, and (2) the structure of the chitosan film is stable once the film is deposited, which keeps the MNPs in place.[3] Microscopic images in Figure S5 in the Supporting Information provide evidence that the morphology of a randomly selected region in a magnetic aligned MNP-chitosan film remains unchanged before and after the removal of MMPs.

In summary, Figure 6 shows that an MNP-chitosan film has the capability of magnetic collection and that magnetic alignment is important for this feature.

3.4.3. Magnetic Attraction and Removal of MMP-EGFP from the Electrodeposited MNP-Chitosan Film. Similar to the phenomenon observed for the cast films, the magnetic attraction and removal of MMP-EGFP can also be observed for electrodeposited films (Figure 6c). The aligned electrodeposited films showed significantly higher working fluorescent signals than those of the chitosan-only film and electrodeposited film without magnetic alignment. After taking away most MMP-EGFP by a strong external magnet, the fluorescent signal of the aligned film was reduced to 8.6% of the working signal. The residual fluorescent signal might arise from nonspecific protein adsorption on the film, as discussed in section 3.4.1. Nonetheless, the magnetic attraction of MMP-EGFP to the aligned electrodeposited MNP-chitosan film and its magnetic removal process demonstrates the potential for multiple cycles of collection and release, a valuable feature of a device interface.

3.5. Collection of Bacteria by the Aligned Electrodeposited MNP-Chitosan Film. *3.5.1. Cell Capture Using Antibody-Functionalized MMPs.* *E. coli* cells were used to study the potential for bacterial capture using antibody-functionalized MMPs. The K-12 *E. coli* wildtype strain

DOI: 10.1021/acsami.5b02339
ACS Appl. Mater. Interfaces 2015, 7, 10587−10598

W3110 was used. Figure 7a demonstrates the coupling of MMPs to an anti-*E. coli* antibody using the EDC method (Experimental Section 2.4). Figure 7b describes the procedure for immunomagnetic separation of the cells. First, *E. coli* were inoculated in 10 mL of Luria Broth growth medium (Alfa Aesar) and grown at 37 °C at 250 rpm shaking until an OD_{600} of 1.0 was reached Then, the *E. coli* (20 μL) were diluted in 5 mL phosphate buffered saline (PBS, 0.1 M, pH 7.0), and an MMP-antibody suspension (10 μL) was added. Two microliters of SYTO 9 green fluorescent nucleic acid stain (Life Technologies) was added to the mixtures to visualize the cells. Because of the selective binding of the antibody to the antigen cells, the MMP-antibody was able to specifically capture *E. coli* cells in the sample. After mixing for 15 min, the MMP-antibody and bound *E. coli* cells (MMP-*E. coli* complex) were attracted to the wall of the container by a magnet. The MMP-*E. coli* complexes were washed 3 times by repeated resuspension in 0.1 M sterile PBS and magnetic collection. The washed MMP- *E. coli* complexes were suspended in 0.5 mL of PBS and subjected to fluorescence microscopy. Figure 7c shows the colocalization of MMP-antibody and stained *E. coli* cells, indicating that the *E. coli* cells were captured by the MMP-antibody conjugates. In contrast, *E. coli* cells showed no attachment to the MMPs without antibody conjugation.

3.5.2. Collection of MMP-E. coli Complexes Using Magnetically Aligned MNP-Chitosan Films. To explore the feasibility of the MNP-chitosan film as a reversible biologically based magnetic particle collector, the assembly and release of the MMP-*E. coli* complex by the electrodeposited MNP-chitosan film is demonstrated. Figure 7d is a schematic illustration of the collection and release of MMP-*E. coli* complexes by MNP-chitosan films. It depicts (1) the magnetic attraction of MMP-*E. coli* complexes by the electrodeposited MNP-chitosan film with magnetic alignment and (2) magnetic removal of MMP-*E. coli* complexes from the film by a stronger external magnet. Similar to the process of the MMP-EGFP application, the MMP-*E. coli* complex suspension was flowed on the surface of the films. After 30 s, the films were rinsed with water 3 times, and their fluorescent signals were examined. It can be seen in Figure 7e that remarkably higher retention of MMP-*E. coli* complexes was observed on the magnetically aligned MNP-chitosan film than on the controls (nonaligned film and chitosan-only film).

To release the MMP-*E. coli* complexes from the magnetically aligned film, we placed the films in water adjacent to a magnet (5 mm away). All of the films were subjected to microscopic imaging for fluorescent signals. In Figure 7e, the fluorescent signals of MMP-*E. coli* complexes in the magnetically aligned film were greatly reduced. These results show the importance of being able to control the rapid collection and release of biological material in a small localized environment (e.g., a microfluidic device interface).

4. CONCLUSIONS

Here, we studied cathodic codeposition of a suspension of chitosan and Fe_3O_4 nanoparticles and observed that the simultaneous imposition of a magnetic field during codeposition can (i) organize structure, (ii) confer magnetic properties, and (iii) yield magnetic films that can perform reversible collection/assembly functions. As a proof of concept, we demonstrated that the magnetic Fe_3O_4-chitosan films can reversibly collect/assemble magnetic particles that had been functionalized with proteins. We envision such magnetic films could have broad generic applications. For instance, magnetic chitosan films could provide a generic means to assemble enzyme-functionalized magnetic beads for biosensing applications. Alternatively, antibody-functionalized magnetic beads could be used to capture cells from a sample while magnetic collection could provide a means to separate and analyze these cells (e.g., for pathogen detection).

From a fabrication standpoint, this work demonstrates that top-down assembly methods using orthogonal cues (electrical and magnetic) can be coupled with bottom-up self-assembly to create soft matter with complex structure and properties. Importantly, fabrication of the magnetic Fe_3O_4-chitosan film is simple, rapid, and reagentless.

■ ASSOCIATED CONTENT

Ⓢ Supporting Information

Detailed synthesis procedures and characterization of the MNPs and MMPs, procedures of conjugating enhanced green fluorescent protein (EGFP) to MMPs, SEM images of MNPs and MMPs, magnetic hysteresis loops of MNPs and MMPs, X-ray diffraction patterns of the MNPs and MMPs, representative in-plane and out-of-plane hysteresis loops of cast and electrodeposited MNP-chitosan films with magnetic alignment, scheme of the conjugation of MMPs and EGFP using carboxyl activating agent EDC, bright and EGFP filter images of MMPs with or without conjugation to EGFP, representative fluorescence microscopic images of interactions between MMP-EGFP and cast films and interactions between MMP-EGFP and electrodeposited films, and bright field microscopic images of a randomly selected region in a magnetically aligned MNP-chitosan film before and after repeated magnetic removal of MMPs. The Supporting Information is available free of charge on the ACS Publications website at DOI: 10.1021/acsami.5b02339.

■ AUTHOR INFORMATION

Corresponding Author

*E-mail: wangqin@umd.edu. Phone: (301) 405-8421. Fax: (301) 314-3313.

Present Address

⊥B.Z.: Environmental Microbial and Food Safety Laboratory, United States Department of Agriculture, Beltsville, MD 20705, United States

Funding

The authors gratefully acknowledge financial support from the USDA-National Institute of Food Agriculture (No: 2014-67021-21585), National Science Foundation (CBET-1435957, CBET-1264509, CBET-1160005), and the Department of Defense, and Defense Threat Reduction Agency (HDTRA1-13-1-0037).

Notes

The authors declare no competing financial interest.

■ ACKNOWLEDGMENTS

We acknowledge the support of the Maryland NanoCenter. Appreciation goes to Zi Teng, Juan Pablo Hurtado Padilla, and Dr. Wen-An Chiou for their professional assistance for the SEM imaging. Appreciation also goes to Dr. Peter Zavalij for his kind interpretation of the X-ray diffraction results.

■ ABBREVIATIONS

MNPs, magnetic nanoparticles

DOI: 10.1021/acsami.5b02339
ACS Appl. Mater. Interfaces 2015, 7, 10587−10598

MMPs, magnetic microparticles
PDMS, polydimethylsiloxane
SEM-EDS, scanning electron microscopy with energy dispersive X-ray spectroscopy analysis
VSM, vibrating sample magnetometry
EGFP, enhanced green fluorescent protein
EDC, 1-ethyl-3-(3-(dimethylamino)propyl) carbodiimide
MES, 2-(*N*-morpholino)-ethanesulfonic acid
Ab, antibody
M_r, remanent magnetization
M_s, saturation magnetization
H_c, coercivity
m_s, the saturation magnetic moment
CS, chitosan
IP, in-plane
OOP, out-of-plane

REFERENCES

(1) Rybtchinski, B. Adaptive Supramolecular Nanomaterials Based on Strong Noncovalent Interactions. *ACS Nano* **2011**, *5* (9), 6791−6818.
(2) Moore, J. S.; Kraft, M. L. Chemistry - Synchronized Self-assembly. *Science* **2008**, *320* (5876), 620−621.
(3) Cheng, Y.; Gray, K. M.; David, L.; Royaud, I.; Payne, G. F.; Rubloff, G. W. Characterization of The Cathodic Electrodeposition of Semicrystalline Chitosan Hydrogel. *Mater. Lett.* **2012**, *87*, 97−100.
(4) Ladet, S.; David, L.; Domard, A. Multi-membrane Hydrogels. *Nature* **2008**, *452* (7183), 76−79.
(5) Xiong, Y.; Yan, K.; Bentley, W. E.; Deng, H.; Du, Y.; Payne, G. F.; Shi, X. W. Compartmentalized Multilayer Hydrogel Formation Using a Stimulus-Responsive Self-Assembling Polysaccharide. *ACS Appl. Mater. Interfaces* **2014**, *6* (4), 2948−2957.
(6) Dai, H. J.; Li, X. F.; Long, Y. H.; Wu, J. J.; Liang, S. M.; Zhang, X. L.; Zhao, N.; Xu, J. Multi-Membrane Hydrogel Fabricated by Facile Dynamic Self-Assembly. *Soft Matter* **2009**, *5* (10), 1987−1989.
(7) Ladet, S. G.; Tahiri, K.; Montembault, A. S.; Domard, A. J.; Corvol, M. T. M. Multi-Membrane Chitosan Hydrogels as Chondrocytic Cell Bioreactors. *Biomaterials* **2011**, *32* (23), 5354−5364.
(8) He, M.; Zhao, Y. T.; Duan, J. J.; Wang, Z. G.; Chen, Y.; Zhang, L. N. Fast Contact of Solid-Liquid Interface Created High Strength Multi-Layered Cellulose Hydrogels with Controllable Size. *ACS Appl. Mater. Interfaces* **2014**, *6* (3), 1872−1878.
(9) Wu, L. Q.; Gadre, A. P.; Yi, H. M.; Kastantin, M. J.; Rubloff, G. W.; Bentley, W. E.; Payne, G. F.; Ghodssi, R. Voltage-Dependent Assembly of The Polysaccharide Chitosan onto an Electrode Surface. *Langmuir* **2002**, *18* (22), 8620−8625.
(10) Redepenning, J.; Venkataraman, G.; Chen, J.; Stafford, N. Electrochemical Preparation of Chitosan/Hydroxyapatite Composite Coatings on Titanium Substrate. *J. Biomed. Mater. Res., Part A* **2003**, *66* (2), 411−416.
(11) Luo, X. L.; Xu, J. J.; Du, Y.; Chen, H. Y. A Glucose Biosensor Based on Chitosan-Glucose Oxidase-Gold Nanoparticles Biocomposite Formed by One-Step Electrodeposition. *Anal. Biochem.* **2004**, *334* (2), 284−289.
(12) Luo, X. L.; Xu, J. J.; Wang, J. L.; Chen, H. Y. Electrochemically Deposited Nanocomposite of Chitosan and Carbon Nanotubes for Biosensor Application. *Chem. Commun.* **2005**, *16*, 2169−2171.
(13) Pang, X.; Zhitomirsky, I. Electrodeposition of Composite Hydroxyapatite-Chitosan Films. *Mater. Chem. Phys.* **2005**, *94* (2−3), 245−251.
(14) Zangmeister, R. A.; Park, J. J.; Rubloff, G. W.; Tarlov, M. J. Electrochemical Study of Chitosan Films Deposited from Solution at Reducing Potentials. *Electrochim. Acta* **2006**, *51* (25), 5324−5333.
(15) Fernandes, R.; Wu, L. Q.; Chen, T. H.; Yi, H. M.; Rubloff, G. W.; Ghodssi, R.; Bentley, W. E.; Payne, G. F. Electrochemically Induced Deposition of a Polysaccharide Hydrogel onto A Patterned Surface. *Langmuir* **2003**, *19* (10), 4058−4062.
(16) Cheng, Y.; Luo, X. L.; Betz, J.; Buckhout-White, S.; Bekdash, O.; Payne, G. F.; Bentley, W. E.; Rubloff, G. W. In Situ Quantitative Visualization and Characterization of Chitosan Electrodeposition with Paired Sidewall Electrodes. *Soft Matter* **2010**, *6* (14), 3177−3183.
(17) Liu, Y.; Zhang, B.; Gray, K. M.; Cheng, Y.; Kim, E.; Rubloff, G. W.; Bentley, W. E.; Wang, Q.; Payne, G. F. Electrodeposition of a Weak Polyelectrolyte Hydrogel: Remarkable Effects of Salt on Kinetics, Structure and Properties. *Soft Matter* **2013**, *9*, 2703−2710.
(18) Zhang, Y. C.; Ji, C. Electro-Induced Covalent Cross-Linking of Chitosan and Formation of Chitosan Hydrogel Films: Its Application as an Enzyme Immobilization Matrix for Use in a Phenol Sensor. *Anal. Chem.* **2010**, *82* (12), 5275−5281.
(19) Guo, M. Q.; Fang, H. D.; Wang, R.; Yang, Z. Q.; Xu, X. H. Electrodeposition of Chitosan-Glucose Oxidase Biocomposite onto Pt-Pb Nanoparticles Modified Stainless Steel Needle Electrode for Amperometric Glucose Biosensor. *J. Mater. Sci.: Mater. Med.* **2011**, *22* (8), 1985−1992.
(20) Zhao, G.; Xu, J. J.; Chen, H. Y. Fabrication, Characterization of Fe_3O_4Multilayer Film and Its Application in Promoting Direct Electron Transfer of Hemoglobin. *Electrochem. Commun.* **2006**, *8* (1), 148−154.
(21) Bai, Y. H.; Du, Y.; Xu, J. J.; Chen, H. Y. Choline Biosensors Based on a Bi-Electrocatalytic Property of MnO_2 Nanoparticles Modified Electrodes to H_2O_2. *Electrochem. Commun.* **2007**, *9* (10), 2611−2616.
(22) Tangkuaram, T.; Ponchio, C.; Kangkasomboon, T.; Katikawong, P.; Veerasai, W. Design and Development of a Highly Stable Hydrogen Peroxide Biosensor on Screen Printed Carbon Electrode Based on Horseradish Peroxidase Bound with Gold Nanoparticles in the Matrix of Chitosan. *Biosens. Bioelectron.* **2007**, *22*, 2071−2078.
(23) Wang, L.; Bao, J.; Wang, L.; Zhang, F.; Li, Y. One-Pot Synthesis and Bioapplication of Amine-Functionalized Magnetite Nanoparticles and Hollow Nanospheres. *Chem.—Eur. J.* **2006**, *12* (24), 6341−6347.
(24) McRae, S. R.; Brown, C. L.; Bushell, G. R. Rapid Purification of EGFP, EYFP, and ECFP with High Yield and Purity. *Protein Expression Purif.* **2005**, *41* (1), 121−127.
(25) Zhang, Y.; Sun, L.; Fu, Y.; Huang, Z. C.; Bai, X. J.; Zhai, Y.; Du, J.; Zhai, H. R. The Shape Anisotropy in the Magnetic Field-Assisted Self-Assembly Chain-like Structure of Magnetite. *J. Phys. Chem. C* **2009**, *113* (19), 8152−8157.
(26) Kim, E.; Gordonov, T.; Bentley, W. E.; Payne, G. F. Amplified and in Situ Detection of Redox-Active Metabolite Using a Biobased Redox Capacitor. *Anal. Chem.* **2013**, *85* (4), 2102−2108.
(27) Bertotti, G. *Hysteresis in Magnetism: For Physicists, Materials Scientists, and Engineers*; Academic Press: San Diego, CA, USA, 1998; pp 3−6.
(28) Liu, F.; Umlor, M. T.; Shen, L.; Weston, J.; Eads, W.; Barnard, J. A.; Mankey, G. J. The Growth of Nanoscale Structured Iron Films by Glancing Angle Deposition. *J. Appl. Phys.* **1999**, *85* (8), 5486−5488.
(29) Kang, S.; Jia, Z.; Shi, S.; Nikles, D. E.; Harrell, J. Easy Axis Alignment of Chemically Partially Ordered Fept Nanoparticles. *Appl. Phys. Lett.* **2005**, *86* (6), 062503.
(30) Fragouli, D.; Das, A.; Innocenti, C.; Guttikonda, Y.; Rahman, S.; Liu, L.; Caramia, V.; Megaridis, C. M.; Athanassiou, A. Polymeric Films with Electric and Magnetic Anisotropy Due to Magnetically Assembled Functional Nanofibers. *ACS Appl. Mater. Interfaces* **2014**, *6* (6), 4535−4541.
(31) Suliţanu, N. D. Electrochemical Deposition of Novel Nanostructured Magnetic Thin Films for Advanced Applications. *Mater. Sci. Eng., B* **2002**, *95* (3), 230−235.
(32) Ge, S.; Li, C.; Ma, X.; Li, W.; Xi, L.; Li, C. X. Approach to Fabricating Co Nanowire Arrays with Perpendicular Anisotropy: Application of a Magnetic Field During Deposition. *J. Appl. Phys.* **2001**, *90* (1), 509−511.
(33) Chantrell, R.; Bradbury, A.; Popplewell, J.; Charles, S. Particle Cluster Configuration in Magnetic Fluid. *J. Phys. D: Appl. Phys.* **1980**, *13* (7), L119.

DOI: 10.1021/acsami.5b02339
ACS Appl. Mater. Interfaces 2015, 7, 10587−10598

(34) Skomski, R.; Hadjipanayis, G.; Sellmyer, D. J. Effective Demagnetizing Factors of Complicated Particle Mixtures. *IEEE Trans. Magn.* **2007**, *43* (6), 2956−2958.
(35) Krycka, K. L.; Borchers, J. A.; Booth, R. A.; Ijiri, Y.; Hasz, K.; Rhyne, J. J.; Majetich, S. A. Origin of Surface Canting within Fe_3O_4 Nanoparticles. *Phys. Rev. Lett.* **2014**, *113* (14), 147203.
(36) Bulte, D. P.; Langman, R. A. Origins of The Magnetomechanical Effect. *J. Magn. Magn. Mater.* **2002**, *251* (2), 229−243.
(37) Cao, Q.; Han, X.; Li, L. Numerical Analysis of Magnetic Nanoparticle Transport in Microfluidic Systems under The Influence of Permanent Magnets. *J. Phys. D: Appl. Phys.* **2012**, *45* (46), 465001.
(38) Wu, L.-Q.; Lee, K.; Wang, X.; English, D. S.; Losert, W.; Payne, G. F. Chitosan-Mediated and Spatially Selective Electrodeposition of Nanoscale Particles. *Langmuir* **2005**, *21* (8), 3641−3646.
(39) Liu, X.; Hu, Q.; Fang, Z.; Wu, Q.; Xie, Q. Carboxyl Enriched Monodisperse Porous Fe_3O_4 Nanoparticles with Extraordinary Sustained-Release Property. *Langmuir* **2009**, *25* (13), 7244−7248.
(40) Stefanita, C.-G. *Magnetism: Basics and Applications*; Springer: Burlington, MA, USA, pp 21−24.

DOI: 10.1021/acsami.5b02339
ACS Appl. Mater. Interfaces 2015, 7, 10587−10598